



HAL
open science

Tetrahydrofuran in $\text{TiCl}_4/\text{THF}/\text{MgCl}_2$: a Non-Innocent Ligand for Supported Ziegler-Natta Polymerization Catalysts

Etienne Grau, Anne Lesage, Sébastien Norsic, Christophe Copéret, Vincent Monteil, Philippe Sautet

► **To cite this version:**

Etienne Grau, Anne Lesage, Sébastien Norsic, Christophe Copéret, Vincent Monteil, et al.. Tetrahydrofuran in $\text{TiCl}_4/\text{THF}/\text{MgCl}_2$: a Non-Innocent Ligand for Supported Ziegler-Natta Polymerization Catalysts. ACS Catalysis, 2013, 3 (1), pp.52-56. 10.1021/cs300764h . hal-00799544

HAL Id: hal-00799544

<https://hal.science/hal-00799544>

Submitted on 21 Nov 2019

HAL is a multi-disciplinary open access archive for the deposit and dissemination of scientific research documents, whether they are published or not. The documents may come from teaching and research institutions in France or abroad, or from public or private research centers.

L'archive ouverte pluridisciplinaire **HAL**, est destinée au dépôt et à la diffusion de documents scientifiques de niveau recherche, publiés ou non, émanant des établissements d'enseignement et de recherche français ou étrangers, des laboratoires publics ou privés.

Tetrahydrofuran in $\text{TiCl}_4/\text{THF}/\text{MgCl}_2$: a Non-Innocent Ligand for Supported Ziegler-Natta Polymerization Catalysts

Etienne Grau,^{1,2,3} Anne Lesage,⁴ Sébastien Norsic,² Christophe Copéret,^{1*} Vincent Monteil,^{2*} Philippe Sautet^{3*}

1: Department of Chemistry, ETH Zurich, HCI H 229, Wolfgang-Pauli-Strasse 10, 8093 Zurich, Switzerland, 2: Université de Lyon, Univ. Lyon 1, CPE Lyon, CNRS, Laboratoire de Chimie Catalyse Polymères et Procédés (C2P2), LCPP team, Bat 308F, 43 Bd du 11 novembre 1918, 69616 Villeurbanne, France, 3 : Université de Lyon, CNRS, Ecole Normale Supérieure de Lyon, Laboratoire de Chimie, 46 Allée d'Italie, 69364 Lyon Cedex 07, France, 4 : Université de Lyon, CNRS, Ecole Normale Supérieure de Lyon, Centre de RMN à Très Hauts Champs, 5 rue de la Doua, 69100 Villeurbanne, France.

ABSTRACT: While Ziegler-Natta (ZN) polymerization is one of the most important catalytic industrial processes, the atomic-scale nature of the catalytically active surface species remains unknown. Coupling high-resolution solid-state NMR spectroscopy with periodic DFT calculations, we demonstrate that the major surface species in the Ziegler-Natta pre-catalyst corresponds to an alkoxy Ti(IV) surface species, which probably results from the ring opening of THF on a cationic Ti(IV) species.

The current generation of heterogeneous catalytic systems for the production of polyolefins, based on titanium chloride supported on magnesium dichloride referred as Ziegler-Natta (ZN) catalyst, is one of the most advanced industrial applications of catalysis, ensuring very high yields and stereochemical control for the obtained polymer chains.^[1] It is thus not surprising that major research efforts have been directed at the understanding of the structure of the active sites of these complex catalysts, in particular by addressing structure activity/selectivity relationships with the aim to further refine such a process.^[1] However, this remains an unmet challenge since the structure of the active sites has remained elusive. While it is clear that the MgCl_2 -based support is here not merely to disperse the active Ti phase, its specific role as well as the structure of surface Ti species, even prior to activation with alkylaluminum compounds, remain largely unknown at the molecular level despite years of research combining experimental^[2] and theoretical investigations.^[3]

In fact, one of the key steps in generating highly active ZN catalysts is the preparation method of the pre-catalyst prior to its activation by an alkylaluminum compounds (referred to as cocatalyst), which finally triggers the polymerization of olefins. It concerns the preparation of MgCl_2 and its subsequent contact with titanium complexes such as TiCl_4 . Both, mechanical and chemical routes are used to obtain “active” MgCl_2 -supported titanium ZN pre-catalyst.^[1c,d] The latter may involve the reaction of solid MgCl_2 with a Lewis base, typically an alcohol^[4] such as ethanol or an ether^[5] such as tetrahydrofuran (THF). This step is usually followed by a treatment with a large excess of TiCl_4 providing then highly active catalysts.

Here by combining high-resolution solid-state NMR spectroscopy and Density Functional Theory (DFT) periodic calculations, we unravel the atomic structure of Ti surface species in a highly active pre-catalyst, $\text{MgCl}_2/\text{THF}/\text{TiCl}_4$, involved in ZN polymerization of ethylene. We clearly evidence that the nature of Ti species is modified by the interaction with MgCl_2 and THF to give a transient cationic Ti mono-nuclear species, which finally leads to a neutral alkoxy Ti species via the ring opening of THF. Beyond its role as a promoter of MgCl_2 , THF is used here as an in-situ probe to reveal the structure of the Ti surface species, the chemical shift of the α -carbons providing a very sensitive spectroscopic signature.

The ZN pre-catalyst used in this study was prepared as follows: MgCl_2 was stirred in boiling THF during 4 h. A white solid corresponding to $\text{MgCl}_2(\text{THF})_x$ with $x \approx 1.5$ was isolated by decantation and successive washing with heptane. This solid was then contacted with an excess of pure TiCl_4 at 90°C during 2 hours. After decantation, the solid was washed with hot toluene and then heptane yielding a yellow powder, named ZN pre-catalyst in the following. The ZN pre-catalyst was characterized in details as follows. The solid contains 3 %wt of Ti and 27 %wt of THF, thus giving the $\text{MgCl}_2(\text{THF})_{0.56}(\text{Ti})_{0.09}$ average molecular formula and a ratio THF/Ti close to 6. The X-Ray powder diffraction pattern is typical of layered α - MgCl_2 with extensive structural disorder (Fig S1 in Supporting Information). It is noteworthy to mention that the ZN pre-catalyst displays no EPR signal and can be characterized by NMR (vide infra) consistent with the absence of isolated Ti(III) in the pre-catalyst. The ZN pre-catalyst provides a highly active catalyst for polymerization of ethylene after activation by triethylaluminum (TEA): an activity of 5000 gPE.gcat⁻¹.h⁻¹ was measured under standard conditions (7 bars of ethylene and 1 bar of H₂ at 80°C). Polyethylene produced exhibits expected properties (Mn=60000 g/mol, PDI=4.6 and a melting temperature of 135.5°C).

In order to gain insight into the molecular structure of surface species, the ZN pre-catalyst was further analyzed by magic angle spinning (MAS) solid-state NMR spectroscopy. Both, two-dimensional (2D) ¹H-¹³C heteronuclear correlation (HETCOR) (Fig. 1) and 2D proton double-quantum (DQ) single-quantum (SQ) correlation spectroscopy (Fig. S2) were applied. The one-dimensional (1D) carbon-13 cross-polarisation (CP) spectrum displays 6 main peaks: 132, 97, 72, 46, 31 and 25 ppm (Fig. 1, top).

Signals at 72 ppm on one hand (C) and at 31 and 25 ppm (E) on the other hand can be readily assigned to respectively to the α - and β -carbons of THF molecules coordinated on the ZN pre-catalyst. Two well-separated peaks are observed for the α -carbons, indicating distinct environments for these THF molecules. The signal at 132 ppm (A) corresponds to the aromatic ring carbons of adsorbed toluene, used during the washing steps (as expected the addition of toluene on the pre-catalyst increases the intensity of this peak; Fig S3). The resonance of the methyl carbons, expected at about 21 ppm, is likely masked by the signal of the β -carbons of THF. The two other signals at 97 (B) and 46 (D) ppm are unexpected as they are strongly shifted with respect to the resonances of coordinated THF and cannot be readily interpreted.

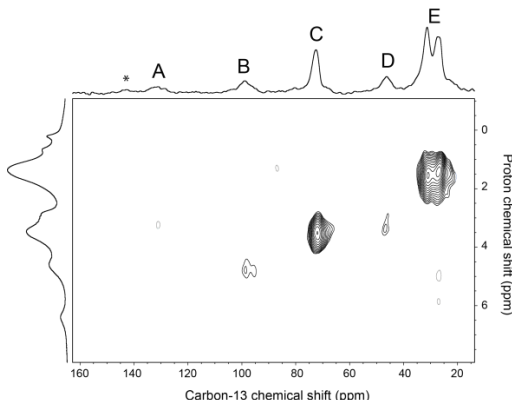


Figure 1. 2D ^1H - ^{13}C HETCOR solid-state NMR spectrum of $\text{MgCl}_2/\text{TiCl}_4/\text{THF}$ ZN pre-catalyst. The 1D ^1H and ^{13}C CPMAS spectra are displayed respectively on the left and on the top of the 2D map. These spectra were recorded at 800 MHz (proton frequency) using a spinning frequency of 22 kHz. Other experimental details are given in the Supporting Information

The 2D ^1H - ^{13}C HETCOR spectrum (Fig. 1) displays four main correlation peaks at $[(\delta^1\text{H}) \text{ ppm}/(\delta^{13}\text{C}) \text{ ppm}]$: [4.7/97], [3.5/72], [3/46] and [1.5/28]. Resonances C and E correlate with protons at around respectively 3.5 and 1.5 ppm respectively, which is in good agreements with the α and β ^1H chemical shifts expected for THF molecules coordinated on the ZN pre-catalyst. A HETCOR spectrum recorded with a longer CP contact time (Fig. S4) shows the expected long-range correlations between the α and β resonances of the coordinated THF. Two clear correlations are also observed for peaks B and D with protons at around respectively 4.7 and 3 ppm. These two proton resonances can be unambiguously assigned to THF α protons from a 2D ^1H DQ-SQ correlation spectrum recorded at 60 kHz MAS (Fig S2, a). Indeed clear correlations are observed at $(\omega_{\text{DQ}}/\omega_{\text{SQ}})=(6.3/4.7)$ and $(6.3/1.6)$ ppm on the one hand and at $(\omega_{\text{DQ}}/\omega_{\text{SQ}})=(4.6/1.6)$ ppm on the other hand, i.e., correlations between these proton resonances at 4.7 and 3 ppm and the intense peak at 1.6 ppm corresponding to the β protons of THF. Thus, on the carbon-13 spectrum, while resonances C corresponds to the α -carbons of adsorbed THF molecules, peaks B and D are attributed to α resonances of additional, unexpected, surface species. Note, that as expected, strong correlations are also observed in the 2D ^1H DQ-SQ spectrum between the α and β protons of the THF molecules adsorbed on the pre-catalyst at $(4.9/3.5)$ and $(4.9/1.4)$ ppm, as well as weak cross-peaks at $(8.1/6.4)$ and $(8.1/1.7)$ ppm between the two proton resonances of adsorbed toluene (Fig. S2, b). In addition, all proton resonances display strong autocorrelation peaks as they all correspond to CH_2 groups. Purely based on chemical shifts, B is reminiscent of the α -carbon of THF coordinated to a cationic Ti center,^[6] while D would be in line with a methylene carbon in α of a chlorine atom; one possibility

would be that this results from the presence of a 4-chloro-butan-1-oxy derivatives originating from the possible ring opening of THF upon interaction of TiCl_4 with $\text{MgCl}_2\text{-THF}$.

To confirm this hypothesis and determine the exact nature of the Ti surface complexes, we explored via periodic DFT calculations the stability of species resulting from the interactions between THF and TiCl_4 on MgCl_2 and calculated the NMR signatures of the corresponding surface species.

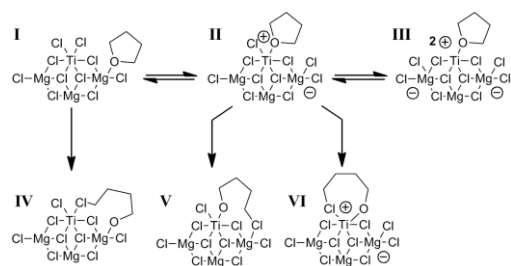


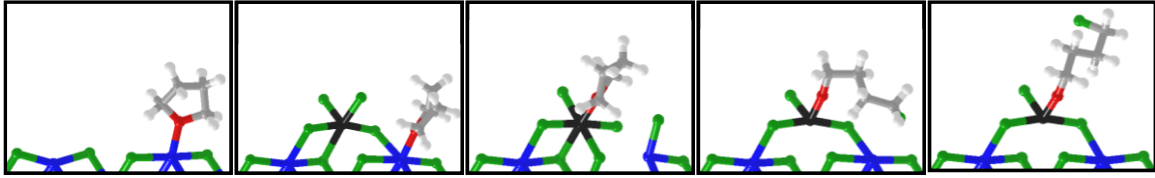
Figure 2. Schematic structure for the Ti surface species and possible mechanisms for THF opening

Numerous surface species can be present on the pre-catalyst (Fig. 2): THF coordinated to Mg (I), THF coordinated to Mg close to Ti (II), THF coordinated to cationic Ti^+ (III) or even THF coordinated to dicationic Ti^{2+} (III) as well as 4-chloro-butan-1-oxy coordinated to Mg (IV), Ti (V) or Ti^+ (VI).

The structures of such species were investigated by adsorbing THF and/or TiCl_4 on periodic models of the (001), (104) and (110) surfaces of $\alpha\text{-MgCl}_2$, and the corresponding NMR chemical shifts were then calculated using $(\text{MgCl}_2)_{10}$ clusters. MgCl_2 bulk and surfaces were calculated (Fig. S5 and Table S1) with the PW91 GGA exchange-correlation functional together with the Grimme method to describe Van der Waals interactions between MgCl_2 layers, using the VASP implementation.^[7] A cut-off energy of 400 eV for the plane-wave basis set provided converged energies. Coordination of THF and TiCl_4 was investigated on the (104) and (110) surfaces (Fig. S6). In agreement with previous studies,^[3a,1] a much more favourable adsorption was found on the (110) surface of $\alpha\text{-MgCl}_2$. As a consequence, this surface was used for further study of the co-adsorption of THF and TiCl_4 . In all surface calculations, a (3×1) supercell containing 9 surface Mg, a 10 layer thick MgCl_2 slab with the first 5 being relaxed, and a vacuum of 10 Å between slabs were used (Fig. S7). In a second step a $(\text{MgCl}_2)_{10}$ cluster was extracted in order to perform calculations of nuclear magnetic shielding tensors using Gaussian09 with the B3PW91 hybrid functional and a high quality 6-311++G(d) basis set.^[8]

In Table 1 are summarized the relative energies and the ^1H and ^{13}C NMR chemical shifts changes with respect to free THF molecules for the different THF and TiCl_4 co-adsorption species on the MgCl_2 (110) surface. THF prefers (with a gain of 11 $\text{kJ}\cdot\text{mol}^{-1}$) to be coordinated to a Mg adjacent to a neutral Ti site (I) than far from it, indicating that the Lewis acidity of Mg is enhanced by the Ti center.^[9] In both cases the ^{13}C and ^1H chemical shifts are mostly unchanged. These data are thus consistent with the assignment of resonances C and E correlation to THF coordinated to Mg whether close or far from a Ti center.

Table 1. Calculated co-adsorption energies for different THF and TiCl₄ species on MgCl₂ (110), differential adsorption energies ($\Delta\Delta E$) and ¹³C and ¹H NMR chemical shifts versus free THF. The energy references are THF in TiCl₄(THF)₂ and TiCl₄ in gas phase for THF and TiCl₄ respectively. Color chart: in blue Mg atom, green Cl, black Ti, red O, gray C, pale gray H.



| | ∞ separated THF, Ti/Mg (0) | THF/Mg (I) | THF/Ti (II) | 4-chloro-butan-1-ol /Ti (V) | Dangling 4-chloro- butan-1-ol /Ti (V') |
|---|---------------------------------------|---------------------------------------|--|--|---|
| E_{ads} (kJ.mol ⁻¹) | -334 | -345 | -269 | -306 | -282 |
| $\Delta\Delta E$ (kJ.mol ⁻¹) | 11 | 0 (ref) | 76 | 39 | 63 |
| ¹³ C NMR shift vs free THF (ppm) | α -O: +1.0 β -O: -1.2 | α -O: +2.6 β -O: +1.7 | α -O: +22.5 β -O: +2.5 | α -O: +21.4 α -Cl: -13.6 β -O: +3.4 β -Cl: +2.9 | α -O: +24.3 α -Cl: -19.2 β -O: +6.1 β -Cl: 5.9 |
| ¹ H NMR shift vs free THF (ppm) | α -O: +0.4 β -O: +0.2 | α -O: +0.6 β -O: +0.3 | α -O: +1.8 β -O: +0.7 | α -O: +1.3 α -Cl: +0.1 β -O: +0.7 β -Cl: +0.0 | α -O: +1.1 α -Cl: +0.0 β -O: +0.6 β -Cl: +0.6 |

The coordination of THF to Ti and the transfer of one of the Cl ligand to an adjacent Mg yield a formally cationic Ti⁺ species (II), which corresponds to an “ate” complex. This ligand permutation from I to II is endoenergetic by 76 kJ.mol⁻¹. From the strong Lewis acidity of the Ti⁺ cation, THF in this species displays significant downfield shifts for the α -nuclei compared to free THF or THF on Mg: namely +20 ppm and +1.5 ppm for α -C and α -H, respectively, while the β -nuclei are barely affected. Such shifts would be consistent with the observed correlation peak at (4.6/97) ppm in the HETCOR spectrum (corresponding to peak B). The displacement of a second Cl ligand leads to the formation of an unstable dicationic Ti species (III); in fact ionic relaxation brings the system back to the mono-cationic species (II). However III can be found as a metastable minimum when two THF are coordinated on Ti giving NMR chemical shifts similar to II (Fig. S8 and Table S2-S3).

So far, none of the calculated species allows the interpretation of the carbon-13 up-field shift observed experimentally for peak D (-25 ppm). In addition cationic species are much less stable than the neutral species such as I (Fig. S8). In view of the possible formation of 4-chloro-butan-1-oxy species by the ring opening of THF, we therefore investigated the corresponding species as depicted in Figure 2 and S8. This process is thermodynamically favoured only from II to V (-37 kJ.mol⁻¹) while the formation of IV (+192 kJ.mol⁻¹) or VI (+147 kJ.mol⁻¹) are highly endoenergetic (Table S2). Note that structures slightly less stable than V, where the chlorine atom of the 4-chlorobutoxy ligand is not coordinated to an adjacent Lewis acid site (Mg) (V') or coordinated to a sublayer Mg atom (V''), can also be proposed.

All these surface complexes are associated with significant NMR chemical shift changes with respect to the reference structure I (Table S3): i) IV induces downfield shifts of approximately 10 ppm for both α - and β -carbons; ii) V displays shifts of +21.4 ppm and -13.6 ppm for the carbons in α of oxygen and chlorine, respectively; iii) VI and V' have chemical shifts similar to V. Of all structures, V' is the only species whose associated calculated chemical shifts

are consistent with the remaining unassigned correlation peak at (3/46) ppm in the HETCOR spectrum (and corresponding to peak D in the 1D ¹³C spectrum). More specifically, the ¹³C calculated shifts with respect to free THF molecules are -19.2 ppm for the carbon in α of chlorine, +24.3 ppm for the one in α of oxygen, +5.9 and +6.1 ppm for the β carbons. This chemical shifts are in good agreement with those observed experimentally for resonances B, D and E respectively. It is noteworthy to mention that the release of the chlorine atom of V to form V' is endoenergetic by +24 kJ.mol⁻¹. The entropic term favours however the pendant chlorine in V' (Fig. S9).

The combination of high-resolution solid-state NMR and periodic calculations thus points out the formation of Ti 4-chlorobutoxy species (especially V') at the surface of MgCl₂/THF/TiCl₄ pre-catalyst. In order to obtain even more direct evidences of the presence of these alkoxy species, a pre-catalyst was prepared by replacing THF by 4-chlorobutan-1-ol (ClBuOH). This MgCl₂/ClBuOH/TiCl₄ pre-catalyst was obtained by contacting with an excess of pure TiCl₄ the corresponding solid support MgCl₂(ClBuOH)_x with $x \approx 1$ using the same receipt described for MgCl₂/THF/TiCl₄ pre-catalyst, and it displayed similar activities (1200 gPE.gcat⁻¹.h⁻¹). The 1D carbon-13 CP spectrum of MgCl₂/ClBuOH/TiCl₄ pre-catalyst displays four main peaks at 96, 48, 45 and 29 ppm while the corresponding support shows three peaks at 63, 45 and 29 ppm (Fig. S10). For the support, the peaks are easily assigned to methylene carbons in α to oxygen (63 ppm), in α to chlorine (45 ppm) and to the methylene carbons in β (29 ppm) of 4-chlorobutan-1-ol adsorbed at MgCl₂ surface. The spectrum of the pre-catalyst clearly demonstrates the formation of Ti 4-chlorobutoxy species as evidenced by the shift of the methylene carbon in α to oxygen from 63 to 96 ppm. The β methylene carbons chemical shifts remain unchanged at 29 ppm while the peak corresponding to the CH₂ in α to chlorine is split into two signals at 45 and 48 ppm (probably depending whether the chlorine atom interact with Ti or not at the pre-catalyst surface). The comparison with the spectrum of MgCl₂/THF/TiCl₄ pre-catalyst further con-

firms that the resonances **B** and **D** at 97 and 46 ppm respectively can be assigned to Ti 4-chlorobutoxy species (**V'**). In fact, alcoholysis of both pre-catalysts yield 1,4-dichlorobutane and traces of 4-chlorobutanol; the former resulted from the acid-catalyzed nucleophilic substitution of the OH by Cl.

While the calculated chemical shifts for species **0**, **I** and **V'** match very well the observed shifts and fully explain the observed NMR spectra, the relative energy for **V'** compared to **I** would predict that **V'** should be only very minor species. Since the experimental system corresponds to a large coverage of THF per surface Ti, we finally explored the effect of additional THF molecules on the relative stability of the various species. Calculations with two to five THF per row of the surface cell (ie for 3 surface Mg and one Ti) were thus performed (Fig. 3, Fig. S8 and Table S2). It should be noted that increasing the THF coverage does not affect the calculated chemical shifts (Table S3).

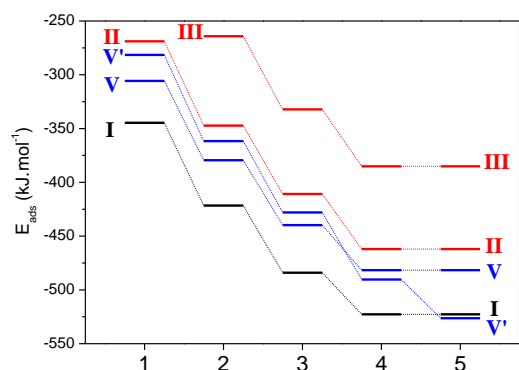


Figure 3. Total adsorption energies of the THF species on MgCl₂ (110) surface for 1, 2, 3, 4 or 5 THF per cell. The energy references are THF in TiCl₄(THF)₂ and TiCl₄ in gas phase for THF and TiCl₄ respectively.

Increasing the surface concentration of THF compared to Ti stabilizes all species investigated. Surprisingly **V'** corresponding to the species with opened THF and a pendant Cl, is also strongly favoured by additional THF making it more stable than **V** at high THF content and slightly more stable than **I**. In view of the experimental conditions (large excess of THF), the comparison of experimental and calculated NMR signatures and the relative energies of possible structures, it is clear that **V'**, a neutral Ti alkoxy species resulting from the ring opening of THF on a cationic Ti center, is a surface species present in MgCl₂/THF/TiCl₄ pre-catalyst. This structure fully explains the ¹³C resonances labelled **B**, **D** and **E**. Moreover, this **V'** species is favoured by the presence of adjacent THF which correspond in large part to resonances **C** and **E**.

In view of the empirical formula for the pre-catalyst - MgCl₂(THF)_{0.56}(Ti)_{0.09} (6 THF per total Ti) - and the presence of NMR signals corresponding to two distinct surface species in a ca. 5-to-1 ratio, the former associated with coordinated THF and the later with ring-opened THF, and the relative stability of surface species based on computational calculations, the data are consistent with the formation of a major Ti alkoxy species (**V'**) having at least 4 THF coordinated on adjacent Mg sites.

In conclusion, the combination of solid-state NMR spectroscopy and periodic calculations has been essential to provide a molecular understanding of the nature of the surface species in MgCl₂/THF/TiCl₄ Ziegler-Natta pre-catalyst. In particular, this study points out that the major surface sites are Ti alkoxy surface species, that result from the opening of THF via cationic Ti/THF transient intermediate, and surrounded by THF coordinated to nearby Mg. In view of the difference of reactivity of alkoxy vs.

chloro titanium compounds towards alkyl aluminium compounds, we are currently investigating how this key Ti alkoxy species impacts the formation and the nature of the active species for the chain-growth in Ziegler-Natta catalysis upon activation.

ASSOCIATED CONTENT

Supporting Information

Text giving experimental details, figures showing X-Rays scattering of pre-catalyst, ¹H DQ-SQ and ¹H-¹³C HECTOR with τ_c=2ms of pre-catalyst, ¹³C CP-MAS of pre-catalyst treated with additional toluene, orthogonal view of different MgCl₂ surface and their energies, orthogonal view of adsorbed THF and TiCl₄ on these surfaces, zoom on different TiCl₄(THF)_{1.5} species on (110) surface and tables of their relative energies and calculated NMR shifts.

AUTHOR INFORMATION

Corresponding Author

* ccoperet@inorg.chem.ethz.ch, monteil@lcpp.cpe.fr, philippe.sautet@ens-lyon.fr.

Author Contributions

Authors conceived and designed the experiments, co-wrote the manuscript, and analyzed the data. E.G, A.L and N.S performed the experiments

ACKNOWLEDGMENT

Authors want to thanks Roger Spitz for his fruitful contribution to Ziegler-Natta catalysis over the years. Financial support from the TGE RMN THC Fr3050 for conducting the research is gratefully acknowledged. Finally, authors thank the PSMN at ENS Lyon where calculations were done.

REFERENCES

- (1) (a) Boor, J. *Ziegler-Natta Catalysis and Polymerization*; Academic Press: New York, 1979. (b) Pino, P.; Mühlaupt, R. *Angew. Chem. Int. Ed.* **1980**, *19*, 857-875. (c) Barbé, P. C.; Cecchin, G.; Noristi, L. *Adv. Polym. Sci.* **1987**, *81*, 1-77. (d) Albizzati, E.; Giannini, U.; Collina, G.; Noristi, L.; Resconi, L. *Catalyst and Polymerizations*, In *Polypropylene Handbook*; Moore, E. P., Ed.; Hanser-Gardner Publications: Cincinnati, OH, 1996; Chapter 2. (e) Mühlaupt, R. *Macromol. Chem. Phys.* **2003**, *204*, 289-327. (f) Kashiwa, N. *J. Polym. Sci. Part A: Polym. Chem.*, **2004**, *42*, 1-8. (g) Eisch, J. J. *Organometallics* **2012**, *31*, 4917-4932.
- (2) (a) Magni, E.; Somorjai, G. A. *Surf. Sci.*, **1996**, *345*, 1-16. (b) Mori, H.; Sawada, M.; Higuchi, T.; Hasebe, K.; Otsuka, N.; Terano, M. *Macromol. Rapid Commun.* **1999**, *20*, 245-250. (c) Kissin, Y. V.; Mink, R. I.; Nowlin, T. E. *J. Polym. Sci., Part A: Polym. Chem.* **1999**, *37*, 4255-4272 (d) Fregonese, D.; Glisenti, A.; Mortara, S.; Rizzi, G. A.; Tondello, E.; Bresadola, S. *J. Mol. Catal. A: Chem.* **2002**, *178*, 115-123 (e) Schmidt, J.; Risse, T.; Hamann, H.; Freund, H.-J. *J. Chem. Phys.*, **2002**, *116*, 10861-10868. (f) Kim, S. H.; Somorjai, G. A. *Proc. Natl. Acad. Sci.*, **2006**, *103*, 15289-15294. (g) Andoni, A.; Chadwick, J. C.; Niemantsverdriet, H. J. W.; Thüne, P. C. *Macromol. Rapid Commun.* **2007**, *28*, 1466-1471. (h) Ribour, D.; Monteil, V.; Spitz, R. *J. Polym. Sci. Part A: Polym. Chem.*, **2008**, *46*, 5461-5470.
- (3) (a) Boero, M.; Parrinello, M.; Terakura, K. *J. Am. Chem. Soc.* **1998**, *120*, 2746-2752. (b) Cavallo, L.; Guerra, G.; Corradini, P. *J. Am. Chem. Soc.* **1998**, *120*, 2428-2436. (c) Toto, M.; Morini, G.; Guerra, G.; Corradini, P.; Cavallo, L. *Macromolecules* **2000**, *33*, 1134-1140. (d) Boero, M.; Parrinello, M.; Hüfner, S.; Weiss, H. *J. Am. Chem. Soc.* **2000**, *122*, 501-509. (e) Martinsky, C.; Minot, C.; Ricart, J. M. *Surf. Sci.* **2001**, *490*, 237-250. (f) Seth, M.; Margl, P.; Ziegler, T. *Macromolecules* **2002**, *35*, 7815-7829. (g) Vanka, K.;

Xu, Z.; Seth M.; Ziegler, T. *Top. Catal.*, **2005**, *34*, 143-164. (h) Busico, B.; Causa, M.; Cipullo, R.; Credendino, R.; Cutillo, F.; Friederichs, N.; Lamanna, R.; Segre, A.; Castelli, V. V. A. *J. Phys. Chem. C*, **2008**, *112*, 1081-1089. (i) Taniike, T.; Terano, M. *Macromol. Rapid Commun.* **2008**, *29*, 1472-1476. (j) Stukalov, D. V.; Zilberberg, I. L.; Zakharov, V. A. *Macromolecules*, **2009**, *42*, 8165-8171. (k) Stukalov, D. V.; Zakharov, V. A. *J. Phys. Chem. C*, **2009**, *113*, 21376-21382. (l) Bahri-Laleh, N.; Correa, A.; Mehdipour-Ataei, S.; Arabi, H.; Haghighi, M. N.; Zohuri, G.; Cavallo, L. *Macromolecules*, **2011**, *44*, 778-783.

(4) (a) Di Noto, V.; Marigo, A.; Viviani, M.; Marega, C.; Bresadola, S.; Zannetti, R. *Makromol. Chem.*, **1992**, *193*, 123-131. (b) Forte, M. C.; Coutinho, F. M. B. *Eur. Polym. J.*, **1996**, *32*, 223-231. (c) Sozzani, P.; Bracco, S.; Comotti, A.; Simonutti, R.; Camurati, I. *J. Am. Chem. Soc.*, **2003**, *125*, 12881-12893. (d) Malizia, F.; Fait, A.; Cruciani, G. *Chem. Eur. J.* **2011**, *17*, 13892-13897.

(5) (a) Kim, I.; Kim, J. H.; Choi, H. K.; Chung, M. C.; Woo, S. I. *J. Appl. Polym. Sci.*, **1993**, *48*, 721-730. (b) Czala, K.; Bialek, M. *Polymer*, **2001**, *42*, 2289-2297. (c) P. Sobata *Coord. Chem. Rev.*, **2004**, *248*, 1047-1060. (d) Seenivasan, K.; Sommazzi, A.; Bonino, F.; Bordiga, S.; Groppo, E. *Chem. Eur. J.*, **2011**, *17*, 8648-8656.

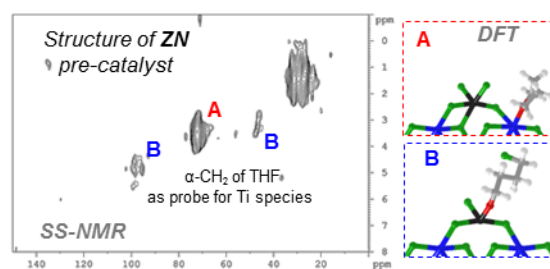
(6) (a) Borkowsky, S. L.; Baezinger, N. C.; Jordan, R. F. *Organometallics* **1993**, *12*, 489-495. (b) Plecnik, C. E.; Liu, F.-C.; Liu, S.; Liu, J.; Meyers, E. A.; Shore, S. G. *Organometallics* **2001**, *20*, 3599-3606.

(7) (a) Kresse, G.; Hafner, J. *Phys. Rev. B*, **1993**, *47*, 558-561. (b) Kresse, G.; Hafner, J. *Phys. Rev. B*, **1994**, *49*, 14251-14269. (c) Kresse, G.; Furthmüller, J. *Comput. Mat. Sci.*, **1996**, *6*, 15-50. (d) Kresse, G.; Furthmüller, J. *Phys. Rev. B*, **1996**, *54*, 11169-11186. (e) Blochl, P. E. *Phys. Rev. B*, **1994**, *50*, 17953-17979. (f) Kresse, G.; Joubert, D. *Phys. Rev. B*, **1999**, *59*, 1758-1775. (g) Grimme, S. *J. Comp. Chem.*, **2006**, *27*, 1787-1799.

(8) *Gaussian 09, Revision A.02*, Frisch, M. J.; Gaussian Inc., Wallingford CT, **2009**.

(9) (a) Negishi, E. *Dalton. Trans.*, **2005**, 827-848. (b) Wang, C.; Zhenfeng, X. *Chem Soc. Rev.*, **2007**, *36*, 1395-1406.

Insert Table of Contents artwork here



Supporting Information

Tetrahydrofuran in $\text{TiCl}_4/\text{THF}/\text{MgCl}_2$: a Non-Innocent Ligand for Supported Ziegler-Natta Polymerization Catalysts

Etienne Grau, Anne Lesage, Sébastien Norsic,
Christophe Copéret,* Vincent Monteil,* Philippe Sautet*

Experimental section

All chemicals were purified using standard Schlenk procedures and handled under argon atmosphere. Solvents were distilled from drying agents. Pure triethylaluminium (TEA) was purchased from Wacko chemical. Ethylene (purity 99.95%) was purchased from Air Liquide and used without any further purification.

Polyethylene characterizations

Molecular weights of polyethylenes were determined by size exclusion chromatography (SEC) using a Waters Alliance GPCV 2000 instrument (columns: PLgel Olexis); two detectors (viscosimeter and refractometer) in trichlorobenzene (flow rate: 1 mL/min) at 150°C. The system was calibrated with polystyrene standards using universal calibration.

Differential scanning calorimetry (DSC) was performed on a Mettler Toledo DSC1 at a heating rate of 5 K/min. Two successive heating and cooling of the samples were performed. We have considered data (T_m values) obtained during the second heats.

ZN Pre-catalyst characterizations

Small-Angle X-ray diffraction (XRD) on powder was carried out on a Bruker D8 Avance diffractometer (33 kV & 45 mA) with Cu $K\alpha$ radiation ($\lambda = 0.154$ nm) in the “Centre de diffractometrie H. Langchambon”, UCBL, Lyon, France. The diffraction patterns were collected in the 2θ angle range [5° - 70°] at a scanning rate of $0.1^\circ/\text{min}$. Analysis of air-sensitive samples were performed using an airtight PMMA dome filled in a glove-box.

GC-MS were performed on Agilent 5973/6890 system using electron impact ionization 70eV, He carrier, 30mx0.25mm HP-INNOWAX capillary column.

EPR analyses were performed in the “Laboratoire de Chimie” at Ecole Normale Supérieure de Lyon on a Bruker Elexys E500 X-Band (9.4 GHz) spectrometer with a standard cavity. The magnetic field is measured on time by a gaussmeter. Analyses of air-sensitive products are performed using quartz Young tubes.

Titanium, Magnesium, Carbon, Hydrogen contents of precatalysts were determined by elemental analysis, performed at the CNRS SCA (Service Central d'Analyse) laboratory in Solaize (France).

Liquid NMR (^1H , ^{13}C , COSY, HSQC) are performed in the “Laboratoire Chimie, Catalyse, Polymère et Procédés” on a Bruker AC300 300MHz at 22°C using standard pulse programs. Spectra were obtained with a 5-mm QNP probe.

Synthesis of pre-catalyst (MgCl₂/THF/TiCl₄)

The Ziegler-Natta pre-catalyst was prepared as follows: first MgCl₂ was stirred in boiling THF (1g of MgCl₂ for 10 mL of THF) for 4 h. Then after cooling down the suspension, heptane was added dropwise. After decantation the filtrate was removed and remaining solid was washed 4 times with heptane. A white powder of MgCl₂(THF)_x with $x \approx 1.5$ was obtained. The compound was then treated with an excess of liquid TiCl₄ (1g of MgCl₂(THF)_x for 10 mL of TiCl₄) at 90°C for 2 h. Toluene was added dropwise, and the mixture cooled down. After decantation, the solid was washed 3 times with hot toluene and 4 times by heptane yielding a yellow powder.

Standard polymerization procedure of ethylene

Caution, all polymerizations involve high pressure and explosive gaz.

Ethylene polymerizations were carried in a 1 L stainless steel autoclave (equipped with safety valves, stirrer, oven) from Sotalem Co.. Before each polymerization, the reactor was washed using a millimolar solution of TEA in heptane. A suspension of few miligrams of pre-catalyst was then prepared in 250 mL of a 3 mM solution of TEA in heptane in a Schlenk tube under argon. The mixture was introduced through cannula into the cooled reactor. Then 1 bar of H₂ was introduced with 7 bars of ethylene. The mixture was heated at 80°C under stirring (500 rpm). During the polymerization the total pressure was maintained constant. After 1 hour of polymerization the reactor was slowly cooled down and degassed. The slurry of polymer was then filtrated, washed with ethanol and dried under vacuum at 90°C.

Solid-State NMR Spectroscopy

All NMR experiments were carried out on a Bruker AVANCE III wide bore spectrometer operating at a ^1H Larmor frequency of 800.13 MHz. The proton spectra were referenced to the single resonance observed in adamantane for protons at 1.87 ppm with respect to neat TMS. ^{13}C chemical shifts were referenced with respect to the CH_2 resonance of adamantane at 38.48 ppm with respect to neat TMS.¹

Heteronuclear correlation spectroscopy

The two-dimensional (2D) proton carbon-13 correlation spectrum of Figure 1 was recorded using a double resonance 2.5 mm probe at a magic angle spinning (MAS) frequency of 22 kHz. A conventional solid-state heteronuclear correlation (HETCOR) experiment was applied, which consists first in a 90° proton pulse, followed by a t_1 evolution period under proton isotropic chemical shift and a cross-polarization (CP) step to transfer magnetization on the neighboring carbon-13 spins. For the spectrum of Figure 1, a total of 128 t_1 increments of 50 μs with 512 scans each were recorded. The total experimental time was 28 hours. The contact time was 500 μs and the repetition delay was 1.5 s. SPINAL-64² heteronuclear decoupling (during t_2) and e-DUMBO-22³ homonuclear decoupling (during t_1) were applied at radio-frequency (RF) fields of respectively 100 kHz and 120 kHz. A ramped CP was used with a proton RF field of 90 kHz at the top of the ramp while the RF field on carbon-13 was adjusted for optimum transfer efficiency. Quadrature detection was achieved using the TPPI method⁴ by incrementing the phase of the proton spin-lock pulse during the CP step. A scaling factor of 0.57 was applied to correct the proton chemical shift scale.

The one-dimensional (1D) carbon-13 spectrum displayed on the top of the 2D map in Figure 1 was recorded using the same experimental conditions and with 18432 scans. For the

spectrum of Figure S6, the contact time was 2000 μs . All other experimental parameters were the same as for Figure 1.

Proton Double-Quantum Spectroscopy

The 2D proton double-quantum (DQ) single-quantum (SQ) correlation spectrum of Figure S4 was recorded at a spinning frequency of 60 kHz using a 1.3 mm triple resonance probe. DQ excitation and reconversion were achieved using the BABA⁵⁻⁷ pulse sequence. A proton 90° pulse of 2.5 μs was used. The length of the excitation and reconversion periods was set to 33.33 μs . Quadrature detection in ω_1 was achieved using the States-TPPI method.⁸ A recycle delay of 1.5 s was used. A total of 300 t_1 increments of 16.67 μs with 128 scans each were recorded. The total experimental time for the DQ experiment was 17 hours.

- (1) Morcombe CR, Zilm KW (2003) Chemical shift referencing in MAS solid state NMR. *J. Magn. Reson.* 162:479-486.
- (2) Fung BM, Khitritin AK, Ermolaev K (2000) An improved broadband decoupling sequence for liquid crystals and solids. *J. Magn. Reson.* 142:97-101.
- (3) Elena B, de Paepe G, Emsley L (2004) Direct spectral optimisation of proton-proton homonuclear dipolar decoupling in solid-state NMR. *Chem. Phys. Lett.* 398:532-538.
- (4) Marion D, Wüthrich K (1983) Application of phase sensitive two-dimensional correlated spectroscopy (COSY) for the measurements of ¹H-¹H spin-spin coupling constants in proteins. *Bioch. Biophys. Res. Com.* 113:967-974.
- (5) Graf R, Demco DE, Gottwald J, Hafner S, Spiess HW (1997) Dipolar couplings and internuclear distances by double-quantum nuclear magnetic resonance spectroscopy in solids. *J. Chem. Phys.* 106:885-895.
- (6) Schnell I, Lupulescu A, Hafner S, Demco DE, Spiess HW (1998) Resolution enhancement in multiple-quantum MAS NMR spectroscopy. *J. Magn. Reson.* 133:61-69.
- (7) Brown SP (2007) Probing proton-proton proximities in the solid state. *Prog. Nucl. Magn. Reson. Spectrosc.* 50:199-251.
- (8) Marion D, Ikura M, Tschudin R, Bax A (1989) Rapid recording of 2D spectra without phase cycling. *J. Magn. Reson.* 85:393-399.

VASP calculation

The DFT calculations were performed in periodic boundary conditions in the Generalized Gradient Approximation (GGA) using Perdew-Wang (PW91) functional, as implemented in the VASP code (version 5.2.11). The Projected Augmented Wave (PAW) method was adopted for the description of atomic cores. In order to take into account Van der Waals interaction (especially between MgCl₂ layers), Grimme method was also implemented. An 10-layer thick slab was used, with an inter-slab distance of approximately 10 Å. The Brillouin zone integration is performed with 1 x 1 x 1 k-point grid generated by the Monkhorst-Pack algorithm. In order to reproduce the properties of extended surfaces, the bottom 5 layers were kept fixed during the calculations at bulk coordinates, while the top layers were allowed to relax.

INCAR file:

```
System = MgCl2+TiCl4+THF

LCHARG = .FALSE.
LVDM = .TRUE.

Grimme method for VdW
VDW_RADIUS = 30.0
VDW_SCALING = 0.75
VDW_D = 20.0
VDW_C6 = 5.71 5.07 10.80 0.70 1.75 0.14
VDW_R0 = 1.364 1.639 1.562 1.342 1.452 1.001

Electronic minimization
PREC = ACCURATE
GGA = 91
EDIFF = 1E-6
ALGO = Fast
LREAL = Auto

Ionic relaxation
EDIFFG = -0.01
NSW = 400
IBRION = 2
POTIM = 0.5
ISIF = 2

DOS related values
ISMEAR = 0
SIGMA = 0.1
```

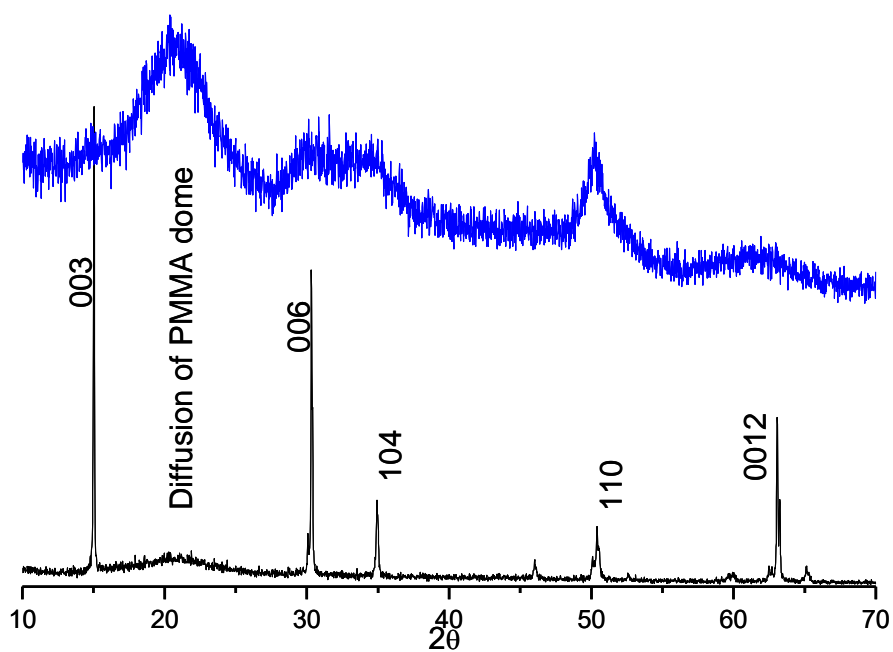


Figure S1. X-rays powder diffraction pattern of MgCl_2 (black bottom curve) and ZN pre-catalyst (blue top curve).

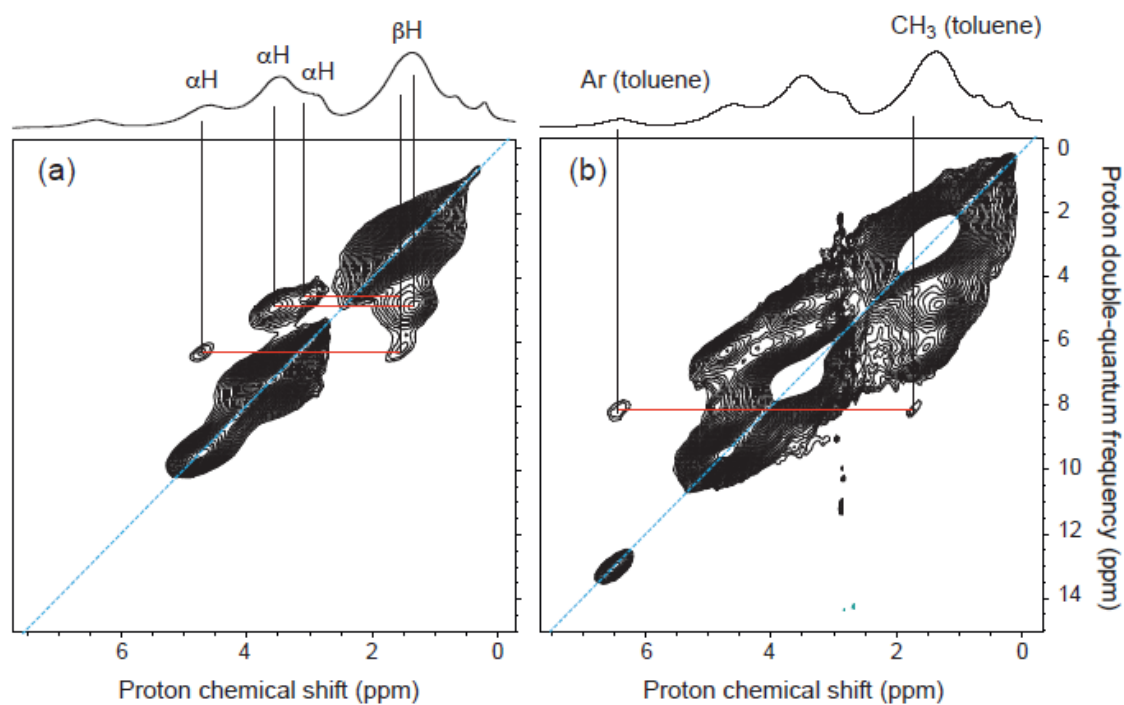


Figure S2. Solid state NMR of $\text{MgCl}_2/\text{TiCl}_4/\text{THF}$ Ziegler-Natta pre-catalyst: Double Quanta ^1H - ^1H 2D-NMR at two different level contour.

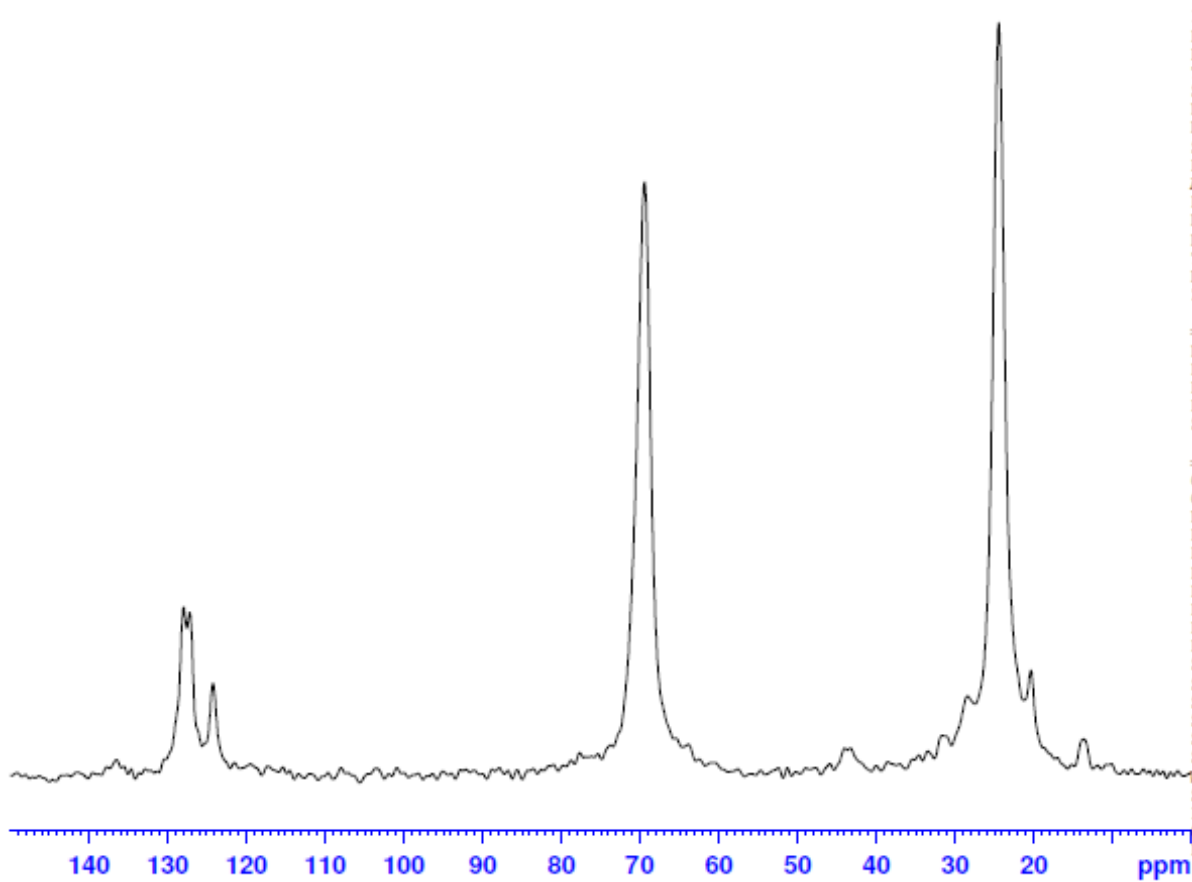


Figure S3. Solid state NMR of $\text{MgCl}_2/\text{TiCl}_4/\text{THF}$ Ziegler-Natta pre-catalyst with additional toluene. Spectrum recorded using 4mm probe at a spinning rate of 10 kHz on a 300MHz Bruker spectrometer.

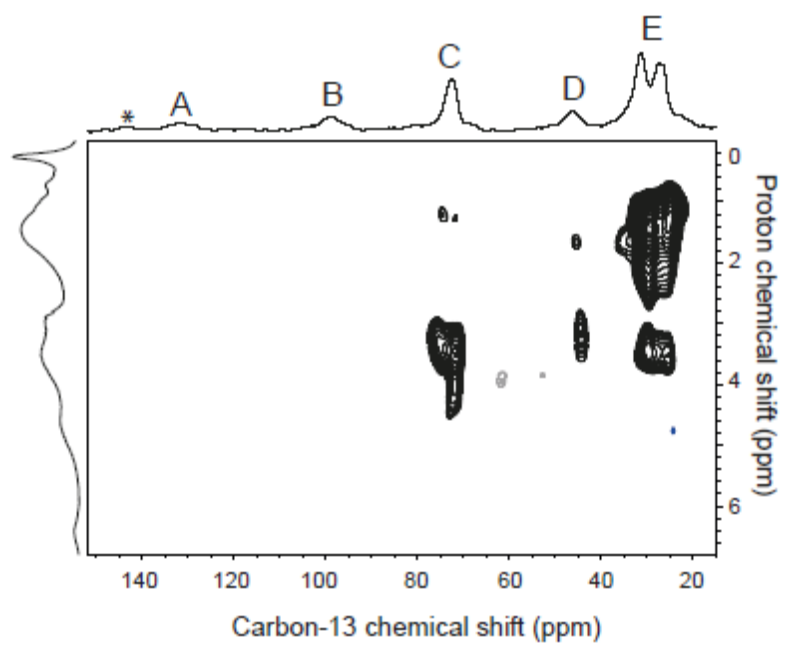
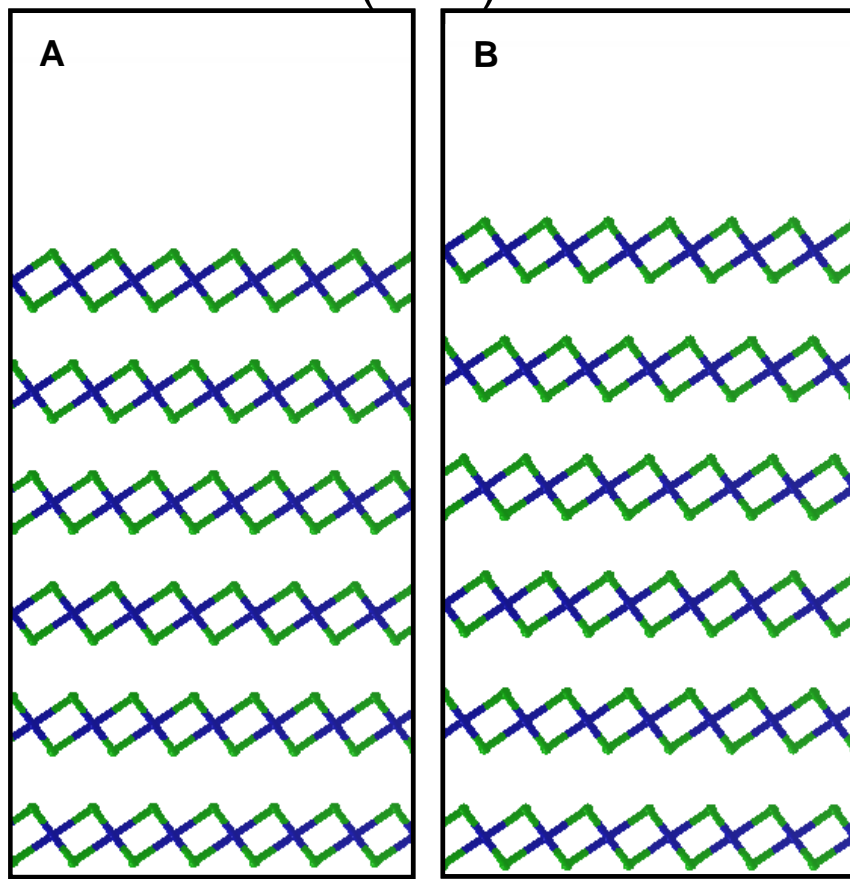
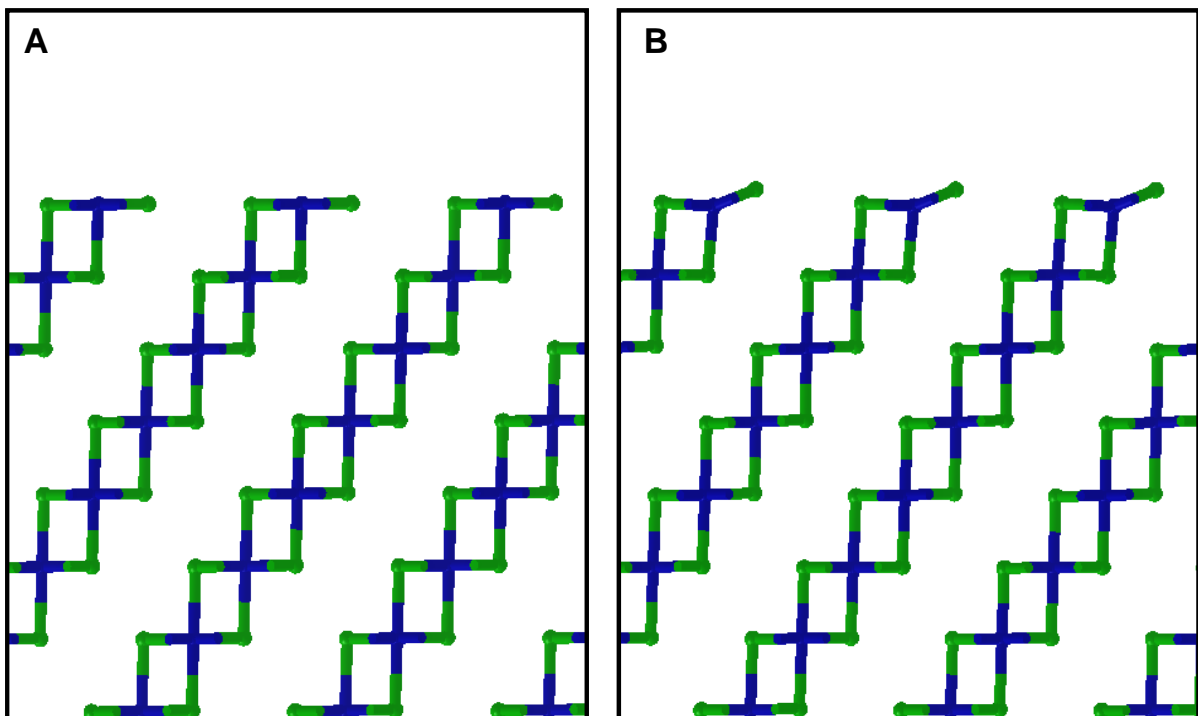


Figure S4. Two-dimensional ^{13}C - ^1H HETCOR spectrum using a cross-polarisation contact time of 2 ms.

(0 0 1)



(1 0 4)



(1 1 0)

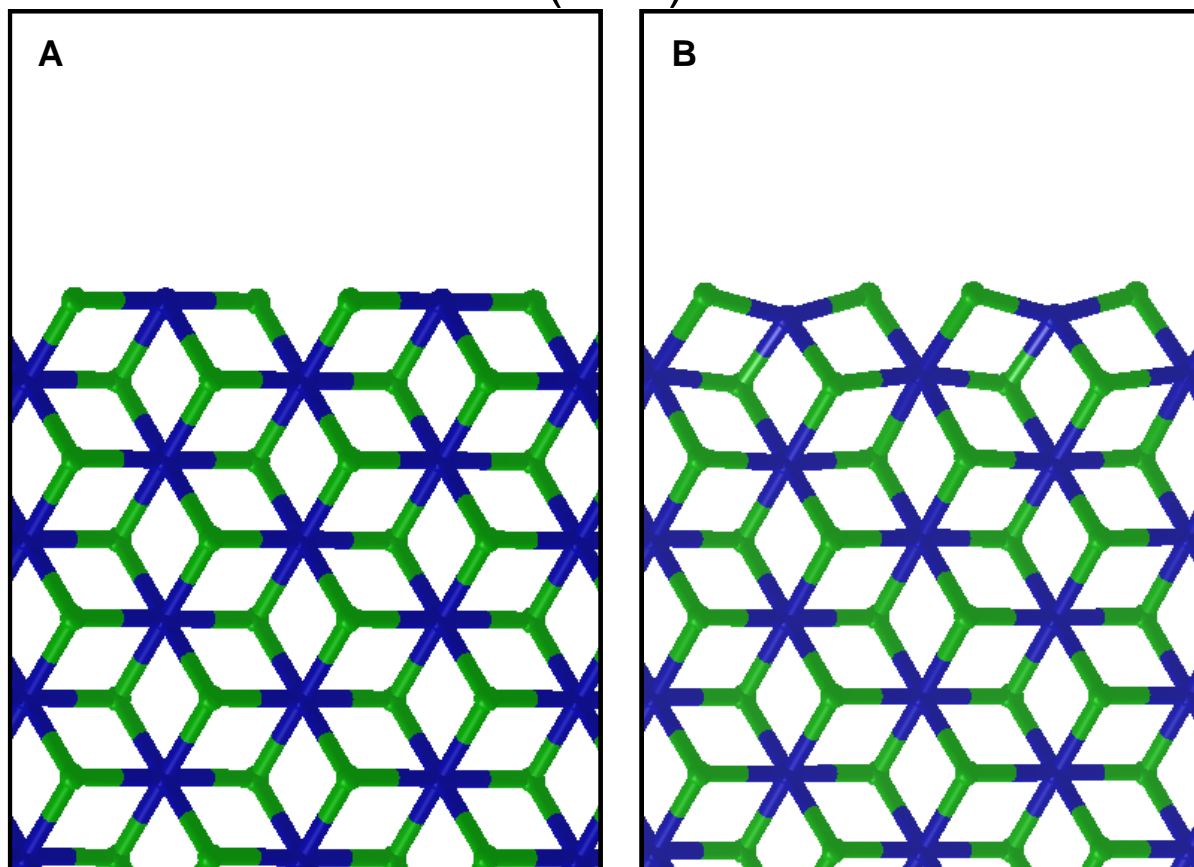


Figure S5. Orthographic view of the structures of the main MgCl_2 crystal surfaces considered in this work: (A) as cut from the bulk, (B) after relaxation.

Table S1: Periodic DFT-calculated surface Energies, γ_{hkl} , of MgCl_2 slab models.

| Surface | (0 0 1) | (1 0 4) | (1 1 0) |
|---|---------|---------|---------|
| γ_{hkl} before ionic relaxation ($\text{J}\cdot\text{m}^{-2}$) | 0.194 | 0.790 | 1.51 |
| γ_{hkl} after ionic relaxation ($\text{J}\cdot\text{m}^{-2}$) | 0.115 | 0.312 | 0.460 |

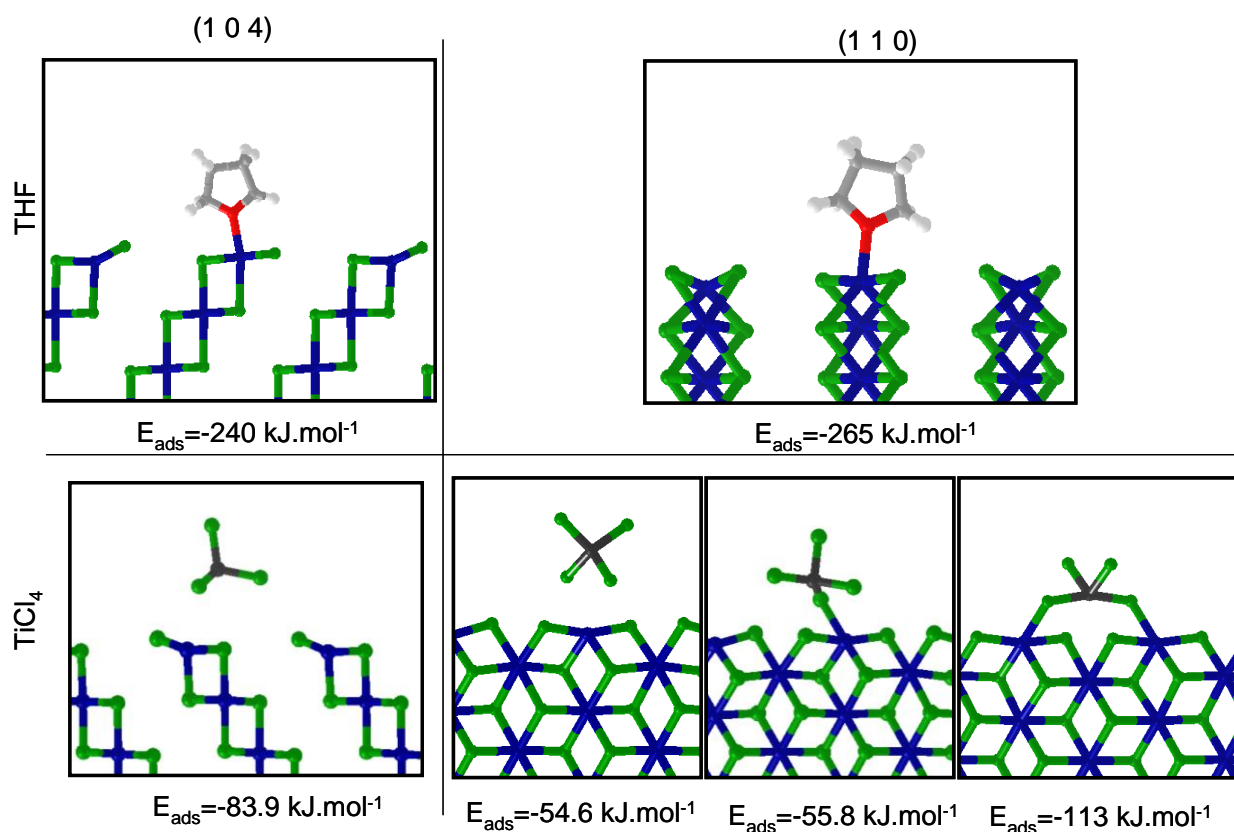


Figure S6. Orthographic view of the structures of the main THF and TiCl_4 adsorption site on MgCl_2 crystal surfaces considered in this work.

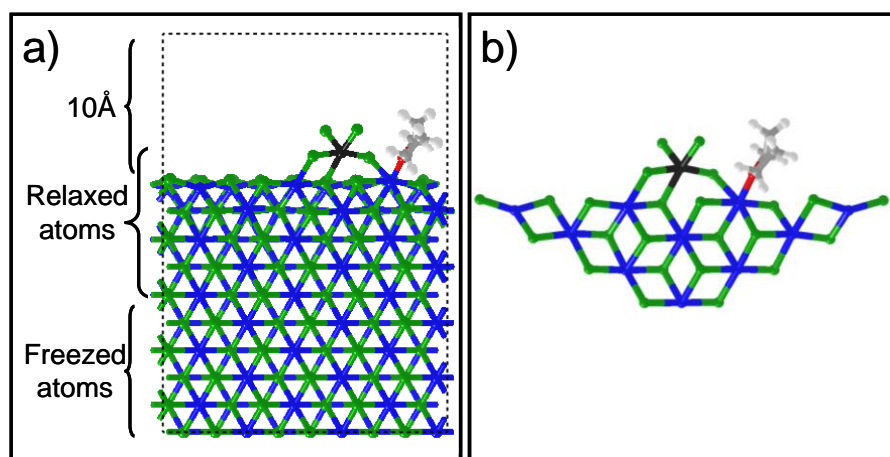
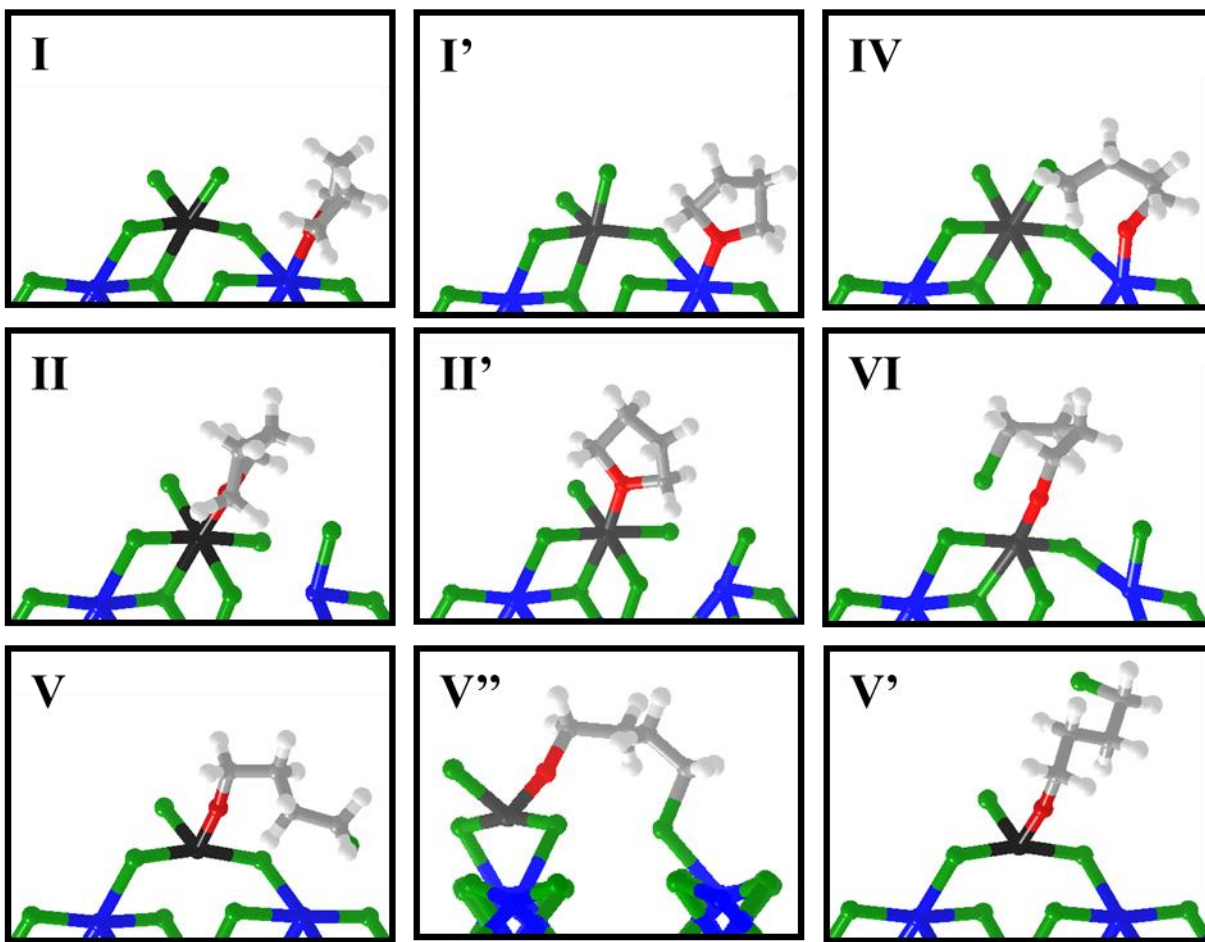
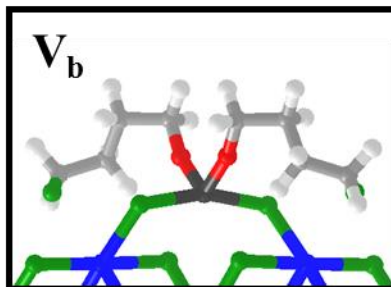
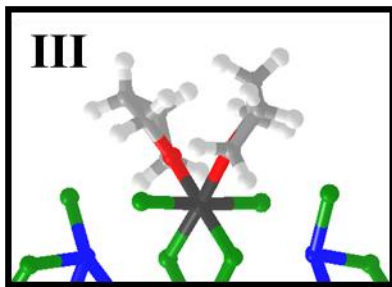
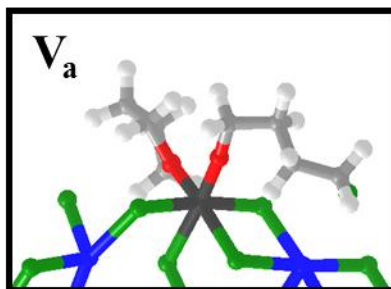
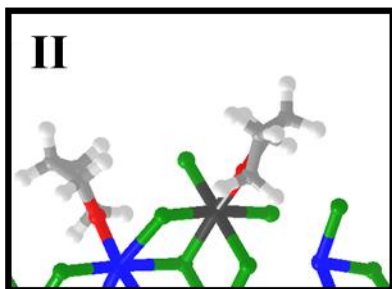
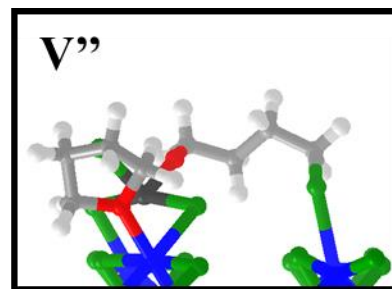
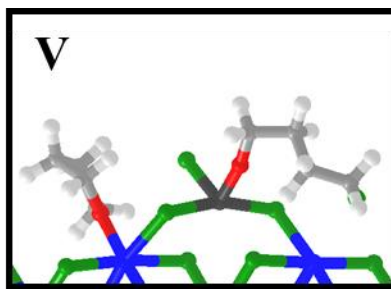
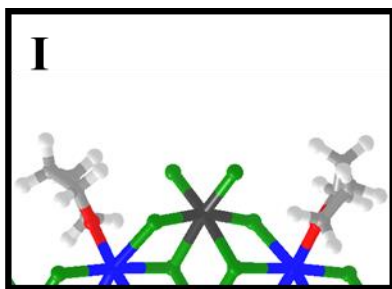


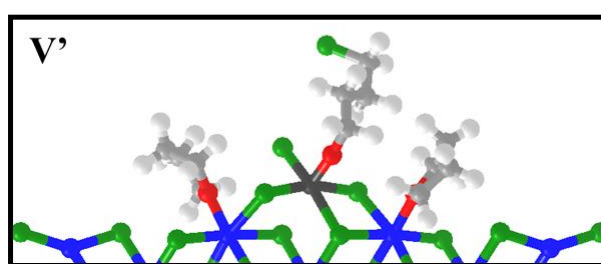
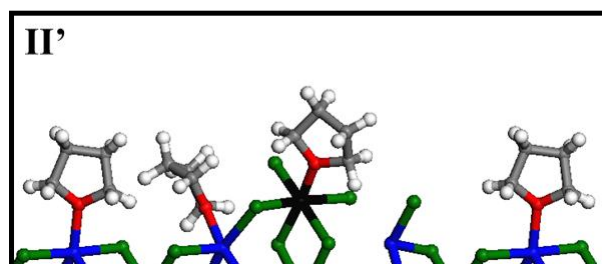
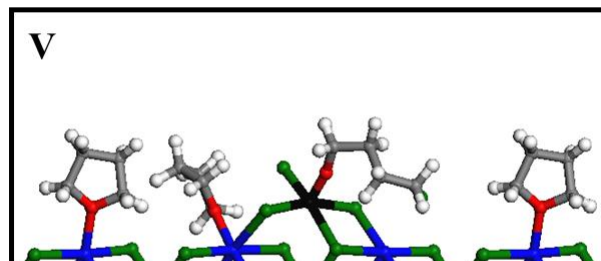
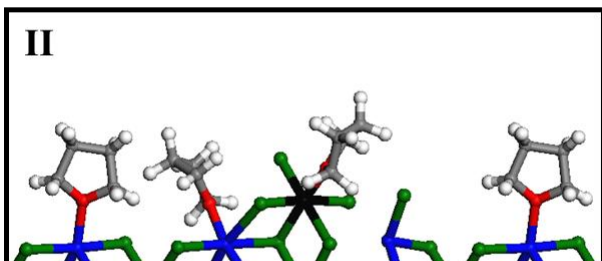
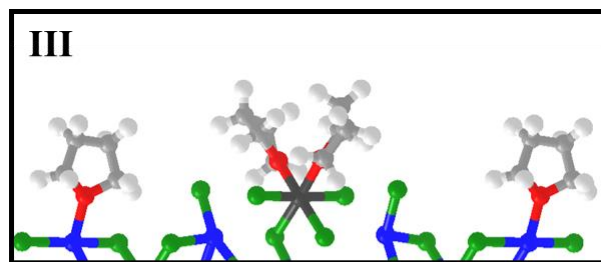
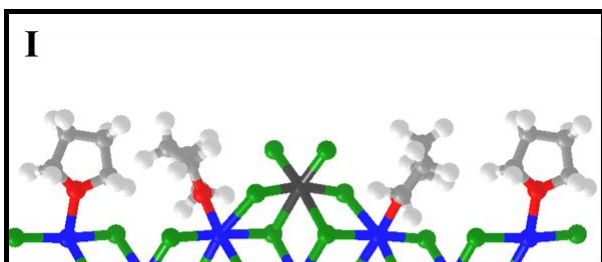
Figure S7. Example of cell (a) and the extracted cluster (b) considered for the calculation of TiCl_4 and THF co-adsorption on MgCl_2 (110) surface (in blue Mg atom, green Cl, black Ti, red O, gray C, pale gray H).



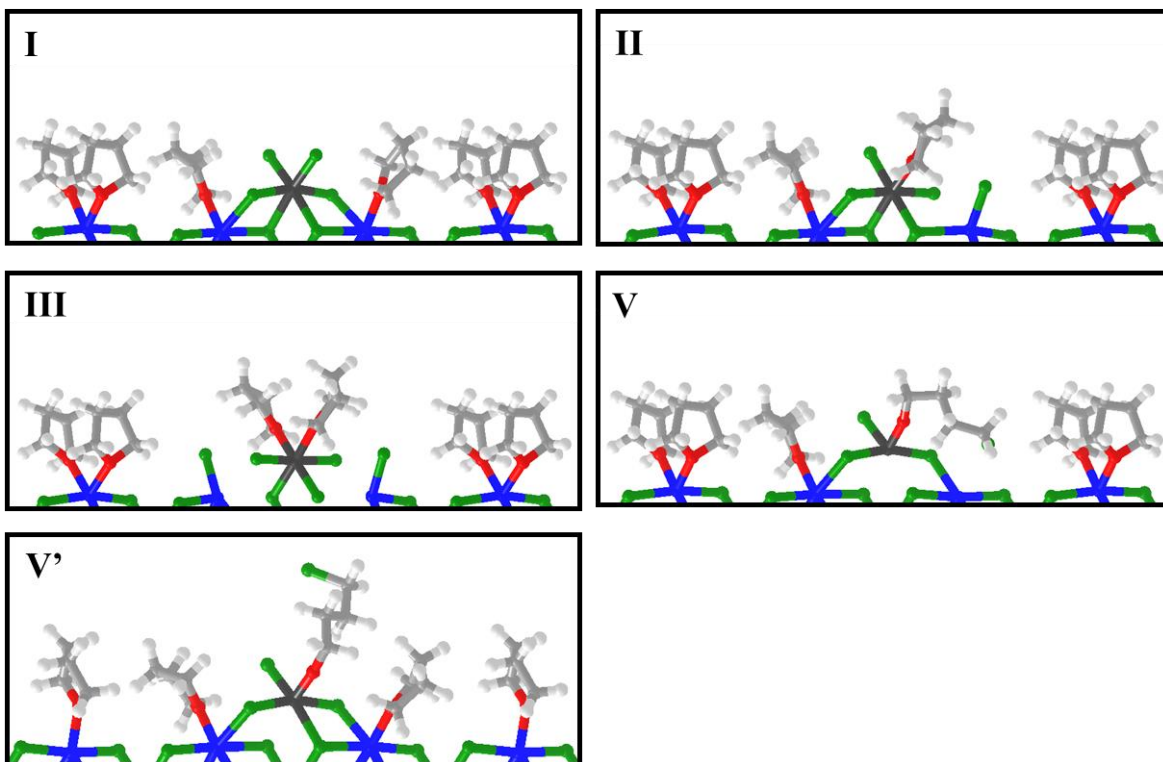
a) 1THF / cell



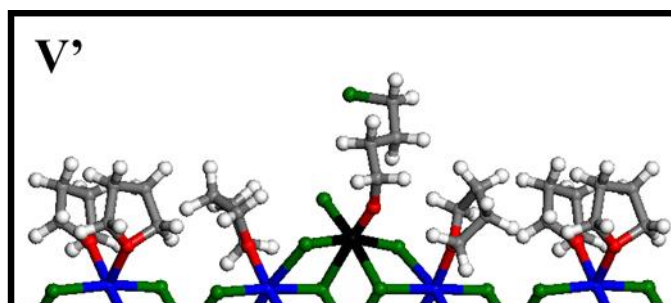
b) 2THF / cell



c) 3THF / cell



d) 4THF / cell



e) 5THF / cell

Figure S8. Orthographic view of the structures of the main THF/ TiCl_4 adsorption site on (110) MgCl_2 crystal surfaces considered in this work.

Table S2: Differential adsorption energies of different THF derivate species vs. **I** in kJ.mol⁻¹.

| Species | 1 THF / TiCl ₄ | 2 THF / TiCl ₄ | 3 THF / TiCl ₄ | 4 THF / TiCl ₄ |
|----------------------|---------------------------|---------------------------|---------------------------|---------------------------|
| I | 0 | 0 | 0 | 0 |
| II | 76 | 74 | 73 | 61 |
| II' | 106 | 108 | 105 | 95 |
| III | not stable | 157 | 152 | 138 |
| IV | 231 | nd | nd | nd |
| V | 39 | 42 | 44 | 41 |
| V' | 63 | 60 | 56 | 32 |
| V'' | 51 | 36 | nd | 1 |
| V_a | - | 117 | nd | 108 |
| V_b | - | 86 | nd | 82 |
| VI | 147 | nd | nd | nd |

nd means not determined

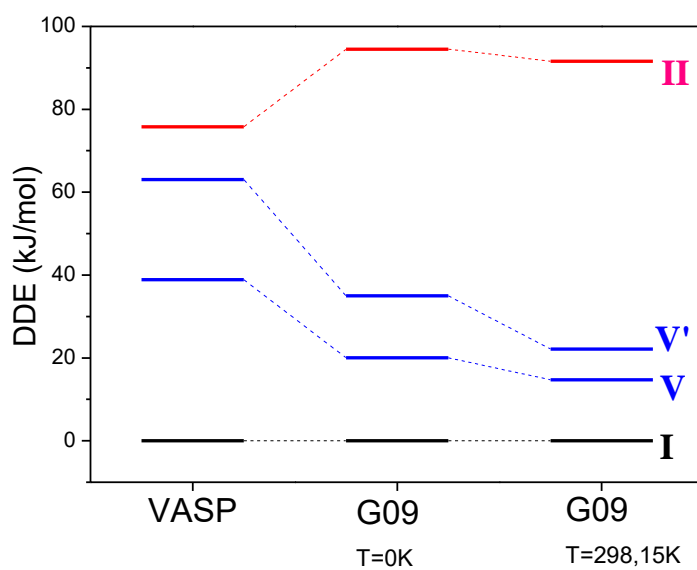


Figure S9. Relative energy of the THF/TiCl₄ species on MgCl₂ (110) using VASP calculation on cell or Thermochemie module of Gaussian09 on cluster at 0K or taking into account vibrational entropy at 298.15K. (It should be noted that the entropy associated to the gain in mobility of the pendant chain is not included in these calculations).

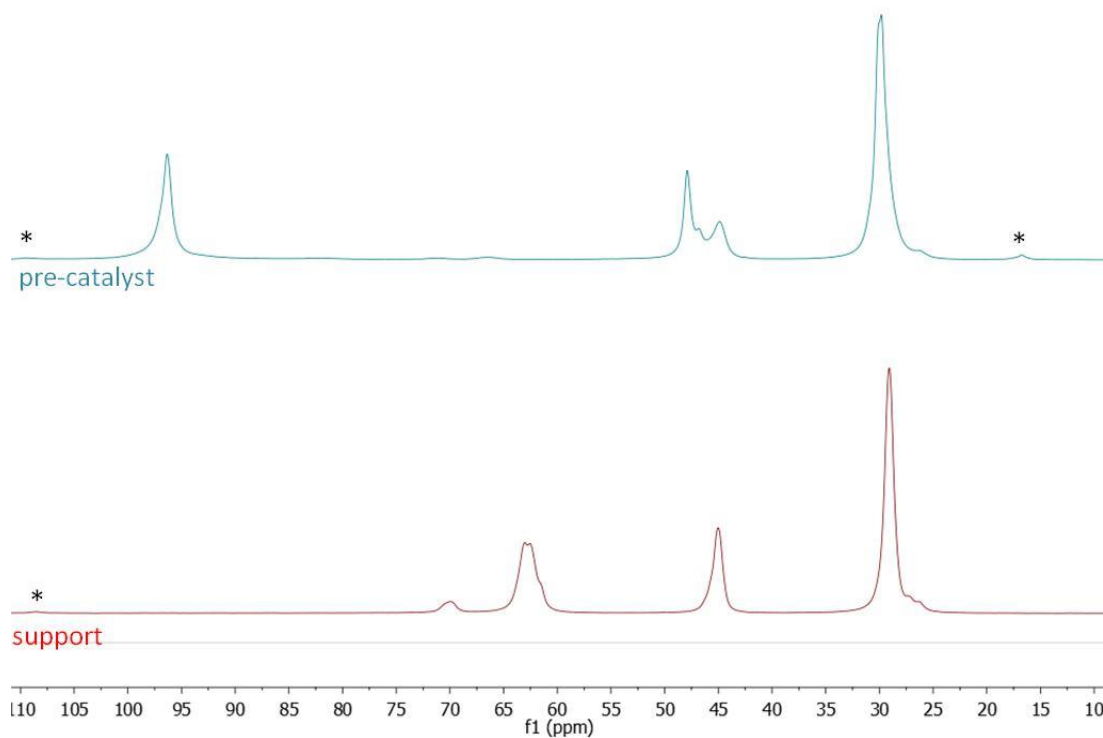


Figure S10. Solid State ^{13}C CP-MAS NMR of solid support $\text{MgCl}_2/\text{ClBuOH}$ (1) and precatalyst $\text{MgCl}_2/\text{TiCl}_4/\text{ClBuOH}$ (2): Spectra recorded using 4mm probe at a spinning rate of 10 kHz on a 500 MHz Bruker spectrometer. Principal peaks are: 63, 45, 29 ppm for $\text{MgCl}_2/\text{ClBuOH}$ (smaller peaks at 27 and 70 ppm corresponds to THF which is present in small amounts in 4-chlorobutanol) and 96, 48, 45, 29 ppm for $\text{MgCl}_2/\text{TiCl}_4/\text{ClBuOH}$.

Table S3: Calculated ^{13}C NMR chemical shifts of different THF derivate species vs free THF.

| Species | α -O (ppm) | α -Cl (ppm) | β -O (ppm) | β -Cl (ppm) |
|---|-------------------|--------------------|------------------|-------------------|
| 1 THF: I' | +7.3 / +5.5 | | +1.2 / +1.0 | |
| 1 THF: II' | +25.0 / 20.5 | | +2.1 / +1.4 | |
| 1 THF: IV | +11.4 | +6.6 | +12.0 | +8.7 |
| 1 THF: V'' | +22.4 | -12.8 | +4.7 | +2.4 |
| 1 THF: VI | +22.3 | -11.2 | +4.4 | -0.3 |
| <hr style="border-top: 1px dashed black;"/> | | | | |
| 2 THF: I | +2.1 | | +1.6 | |
| 2 THF: II | +21.6 (+2.0) | | +2.6 (+1.5) | |
| 2 THF: III | +17.1 | | +2.3 | |
| 2 THF: V | +20.6 (+1.7) | -13.7 | +2.9 (+1.1) | +2.4 |
| 2 THF: V_a | +20.6 (+15.9) | -14.8 | +2.8 (+1.4) | +2.3 |
| 2 THF: V_b | +15.8 | -13.6 | +2.8 | +1.8 |